



UNIVERSITY OF LEEDS

This is a repository copy of *Pyrolysis-catalytic hydrogenation of cellulose-hemicellulose-lignin and biomass agricultural wastes for synthetic natural gas production*.

White Rose Research Online URL for this paper:  
<http://eprints.whiterose.ac.uk/155368/>

Version: Accepted Version

---

**Article:**

Jaffar, MM, Nahil, MA and Williams, PT [orcid.org/0000-0003-0401-9326](https://orcid.org/0000-0003-0401-9326) (2020) Pyrolysis-catalytic hydrogenation of cellulose-hemicellulose-lignin and biomass agricultural wastes for synthetic natural gas production. *Journal of Analytical and Applied Pyrolysis*, 145. ARTN: 104753. ISSN 0165-2370

<https://doi.org/10.1016/j.jaap.2019.104753>

---

© 2019 Elsevier B.V. Licensed under the Creative Commons Attribution-NonCommercial-NoDerivatives 4.0 International License (<http://creativecommons.org/licenses/by-nc-nd/4.0/>).

**Reuse**

This article is distributed under the terms of the Creative Commons Attribution-NonCommercial-NoDerivatives (CC BY-NC-ND) licence. This licence only allows you to download this work and share it with others as long as you credit the authors, but you can't change the article in any way or use it commercially. More information and the full terms of the licence here: <https://creativecommons.org/licenses/>

**Takedown**

If you consider content in White Rose Research Online to be in breach of UK law, please notify us by emailing [eprints@whiterose.ac.uk](mailto:eprints@whiterose.ac.uk) including the URL of the record and the reason for the withdrawal request.



[eprints@whiterose.ac.uk](mailto:eprints@whiterose.ac.uk)  
<https://eprints.whiterose.ac.uk/>

## **Pyrolysis-Catalytic Hydrogenation of Cellulose-Hemicellulose-Lignin and Biomass Agricultural Wastes for Synthetic Natural Gas Production.**

Mohammad M. Jaffar, Mohamad A. Nahil, Paul T. Williams\*

School of Chemical and Process Engineering, University of Leeds, Leeds, LS2 9JT, U.K.

(\*Corresponding author; Email; p.t.williams@leeds.ac.uk; Tel; #44 1133432504)

### **Abstract**

The production of methane from the biopolymers; cellulose, hemicellulose and lignin, and also four different agricultural waste biomass samples was investigated using a two-stage pyrolysis-catalytic hydrogenation reactor. The biomass agricultural waste samples were rice straw, willow, sugar cane bagasse and ugu plant. Pyrolysis of the biomass samples was carried out in a 1<sup>st</sup> stage reactor while the catalytic hydrogenation was carried out the 2<sup>nd</sup> stage reactor using a 10 wt.% Ni/Al<sub>2</sub>O<sub>3</sub> catalyst maintained at 500 °C with heating rate of 20 °C min<sup>-1</sup> and a H<sub>2</sub> space velocity of 3600 ml h<sup>-1</sup> g<sup>-1</sup><sub>catalyst</sub>. The thermal degradation characteristics of the biomass components, mixtures of the components and the biomass waste samples was also conducted using thermogravimetric analysis (TGA). TGA of the mixtures of the biomass components showed interaction, illustrated by a shift in the thermal degradation temperatures for hemicellulose and lignin. The results from the pyrolysis-catalytic hydrogenation revealed that the methane yield increased in the presence of the catalyst; the methane yield obtained from the hemicellulose (7.9 mmol g<sup>-1</sup><sub>biomass</sub>) and cellulose (7.65 mmol g<sup>-1</sup><sub>biomass</sub>) was significantly higher than that produced from lignin, (3.7 mmol g<sup>-1</sup><sub>biomass</sub>). The pyrolysis-catalytic hydrogenation of the mixtures of the biopolymers showed clear interaction, producing higher total gas yield and methane yield compared to calculated values. Pyrolysis-catalytic hydrogenation of the agricultural biomass wastes suggests that the product methane yield was influenced by the percentage of hemicellulose and cellulose content in the biomass.

**Key words:** Biomass; Pyrolysis; Hydrogenation; Methanation; Methane

**Introduction:**

The environmental impact of climate change linked to fossil fuel use has resulted in intense interest in alternate renewable energy fuels. Lignocellulosic biomass is considered to be a major renewable energy resource because of its worldwide abundance and carbon neutrality [1, 2]. Biomass conversion methods include thermochemical conversion and bio-chemical conversion [3-6]. Recently conversion of lignocellulosic biomass into synthetic natural gas (methane) is receiving great interest, mainly because of the already well developed and organized infrastructure and distribution facilities for natural gas [7-8]. Most literature available on methane production from lignocellulosic biomass is carried out using bio-chemical conversion methods [9-11]. However, there are significantly fewer publications related to thermochemical conversion of lignocellulosic biomass to produce methane as substitute natural gas. Pyrolysis of biomass has been used to produce bio-oil, biochar and gas products. The gas products are high in carbon dioxide and carbon monoxide. However, a novel additional process step is to pass the evolved pyrolysis oils and gases as hot vapours directly to a catalytic hydrogenation reactor where the carbon oxides are hydrogenated in the presence of added hydrogen gas.

Several studies have been performed to optimize CO<sub>2</sub> and CO conversion to methane. Heterogeneous catalysts of VIII B group metals such as Ni, Co, Fe, Ru, Rh, Pt, Pd have been investigated [12]. In addition, studies have been performed into the effect of the catalyst support material such as alumina, SiO<sub>2</sub> and MCM-41, and it has been reported that the main drawback of using SiO<sub>2</sub> and MCM-41 supports are their low stability. For example, it has been reported that SiO<sub>2</sub> and MCM-41 sinters in the presence of water derived from the methanation reaction, while alumina is comparatively stable [13-14]. In our previous work comparison of different catalyst metals (Ni, Fe, Co, and Mo) loaded on Al<sub>2</sub>O<sub>3</sub>, SiO<sub>2</sub> and MCM-41 support

material in relation to methane production was investigated. We showed that the highest catalytic activity and selectivity was observed with Ni metal loaded on the alumina support [15]. Similar results have been reported by Aziz et al., [16] where they reported the reduced catalytic activity of Fe and Mo compared to that of Ni. In the literature Ni, Ru and Rh are considered to be highly active and selective for methane production but, because of their higher cost, nickel-based catalysts are preferred.

To further understand the biomass pyrolysis-catalytic hydrogenation process, it is of interest to investigate the influence of the main components of biomass, cellulose, hemicellulose and lignin, on the production of methane. In general, most biomass composition is comprised of between 40-60 wt.% cellulose, 20-40 wt.% hemicellulose and 10-25 wt.% lignin [17]. It has been reported that the different biopolymers decompose over different temperature ranges [5]. Biomass thermal decomposition with increasing temperature involves initial moisture loss, followed by decomposition of hemicellulose, followed by cellulose decomposition and finally lignin decomposes. Also, it has been reported that the pyrolysis of the different biomass components produces a different product slate. For example, lignin pyrolysis yields higher hydrogen and methane yield as compared to that of cellulose and hemicellulose, while higher CO and CO<sub>2</sub> yield are obtained from cellulose and hemicellulose [5].

This research reports on the production of methane using a two-stage pyrolysis-catalytic hydrogenation reactor system from cellulose, hemicellulose and lignin and from four different agricultural biomass wastes. The aim of the work was to identify which of the main biopolymer components of biomass contributes most CH<sub>4</sub> during pyrolysis-catalytic hydrogenation. Mixtures of cellulose, hemicellulose and lignin components in different ratios were also studied to investigate any interaction between the components. In addition, the composition of the biomass wastes was estimated from thermogravimetric analysis and the analysis used to

understand the link between biomass composition and CH<sub>4</sub> yield during pyrolysis-catalytic hydrogenation. The catalyst used for hydrogenation was a 10 wt.% nickel-alumina catalyst. In addition, the published mechanism of the catalytic hydrogenation of carbon oxides has also been discussed.

## **Materials and Methods**

### **2.1 Biomass components and agricultural waste biomass samples**

The three main biomass components, cellulose, hemicellulose (xylan) and lignin were obtained from Sigma-Aldrich Ltd., UK. In addition, four different agricultural waste biomasses consisting of rice straw (Pakistan), sugar cane bagasse (Pakistan), ugu plant (Nigeria) and willow (UK) were investigated. The thermal degradation characteristics of the biomass components and different agricultural biomasses was determined using thermogravimetric analysis using a Shimadzu TGA-50. Elemental analysis (CHNO) was carried out using a Thermos EA2000 Analyzer. The results of ultimate analysis are shown in Table 1. Table 2 shows the proximate analysis of the biomass components and agricultural waste biomasses, determined from TGA.

### **2.2. Catalyst Preparation**

The catalyst used for the pyrolysis-catalytic hydrogenation experiments was 10 wt.% Ni/Al<sub>2</sub>O<sub>3</sub>. Nickel-alumina was chosen as the catalyst because of its reported high activity and selectivity towards methanation reactions [18]. Also, as mentioned before, the highest catalytic activity and selectivity for CH<sub>4</sub> was achieved with the 10wt.% Ni/Al<sub>2</sub>O<sub>3</sub> catalyst as reported in our

previous article [15]. The catalyst used was prepared by wet impregnation method. For the preparation of the catalyst; nickel nitrate hexahydrate  $\text{Ni}(\text{NO}_3)_2 \cdot 6\text{H}_2\text{O}$  from Sigma Aldrich, UK, Ltd was dissolved in 25 ml of deionized water under constant stirring for 30 min to obtain an aqueous solution. The alumina support was then added to the aqueous solution of  $\text{Ni}(\text{NO}_3)_2 \cdot 6\text{H}_2\text{O}$  and stirred continuously for another 30 min at room temperature. The temperature of the slurry was then increased by 15 °C after every 30 min until the water evaporated and a semi-solid slurry precursor catalyst was obtained. This precursor was then dried in an oven overnight at 105 °C followed by calcination at 550 °C in a calcination furnace for 3 h. The calcined catalyst was then ground and sieved to obtain a particle size of 50-212 microns. The catalyst was reduced in a reduction furnace at 800 °C for 2 h in the presence of hydrogen (5 H<sub>2</sub> and 95 % N<sub>2</sub>).

### **2.3. Two-Stage fixed bed pyrolysis-catalytic hydrogenation reactor**

The pyrolysis-catalytic hydrogenation of the cellulose, hemicellulose and lignin and the four biomass samples was carried out in a two stage fixed bed reactor, pyrolysis-catalytic hydrogenation system. In addition, experiments were undertaken with different mixtures of cellulose, hemicellulose and lignin. Pyrolysis of the biopolymers and biomass samples took place in the first stage reactor and the evolved gases and vapors were passed directly to the second stage where catalytic hydrogenation took place in the presence of added hydrogen gas. A schematic diagram of the reactor system is shown in Figure 1. The reactor was constructed of stainless steel with a first stage of dimensions 25 cm long x 5 cm diameter and second stage of dimensions 32 cm long x 2 cm diameter. Each of the two stages were heated by two separate temperature-controlled furnaces. Thermocouples monitored the biomass and catalyst temperatures. The biopolymer or biomass feed stock (1.0 g) was placed in a crucible suspended

in the centre of the first stage pyrolysis reactor and the 10 wt.% Ni/Al<sub>2</sub>O<sub>3</sub>) catalyst (1.0 g) was placed in the second stage reactor and held in place using stainless steel mesh and quartz wool. For comparison, clean washed quartz sand was substituted for the catalyst to determine the effect of pyrolysis-thermal cracking compared with the pyrolysis catalytic hydrogenation with the 10 wt.% Ni/Al<sub>2</sub>O<sub>3</sub> catalyst. Inert carrier gas in the form of nitrogen with a flow rate of 60 ml min<sup>-1</sup> continuously flowed through the reactor system. The hydrogen for the catalytic hydrogenation was supplied directly in the second stage of the reactor by a Packard 9200 Hydrogen generator with a H<sub>2</sub> gas space velocity of 3600 ml h<sup>-1</sup> g<sup>-1</sup><sub>catalyst</sub>. The 2<sup>nd</sup> stage catalyst reactor was heated to 500 °C and once stabilized, the pyrolysis of the biopolymers and biomass was initiated, heating the sample from ambient temperature to a final temperature of 800 °C with heating rate of 20 °C min<sup>-1</sup>. These optimized conditions were selected based on data obtained from our previous report [15]. Dry ice condensers and water-cooled condensers were attached to the output of the reactors to condense the liquid products and the non-condensed gas product was collected in a 25 L Tedlar<sup>TM</sup> gas sample bag. The total reaction time was 65 min, after which the hydrogen was turned off and gas was collected in the gas sample bag for a further 20 min. To validate the experiments, initial experiments were repeated at least twice at 500 °C catalytic bed temperature with the Ni/Al<sub>2</sub>O<sub>3</sub> catalyst. The measured concentrations of CO, CO<sub>2</sub> and CH<sub>4</sub> showed a very low standard deviation with all the biomass components investigated, demonstrating excellent experimental repeatability. For example, standard deviations for CO, CO<sub>2</sub> and CH<sub>4</sub> gas concentrations in the case of lignin feedstock were 0.72, 0.35 and 0.18 respectively. Hemicellulose feedstock showed standard deviations for CO, CO<sub>2</sub> and CH<sub>4</sub> of 0.004, 0.288 and 0.04 respectively. While in the case of cellulose CO, CO<sub>2</sub>, and CH<sub>4</sub> showed standard deviations of 0.049, 0.39 and 0.128 respectively.

#### **2.4. Product Analysis**

The gas product from the pyrolysis-catalytic hydrogenation of the biopolymers and biomass collected in the Tedlar<sup>TM</sup> gas sample bag were analysed immediately after each experiment using packed column gas chromatography (GC). Hydrocarbon product gases were analyzed using a Varian CP-3380 GC equipped with a flame ionization detector (FID), having column dimensions of 2 m long x 2 mm diameter, with 80-100 mesh HayeSep packing and N<sub>2</sub> as a carrier gas. Permanent gases (H<sub>2</sub>, O<sub>2</sub>, N<sub>2</sub> and CO) were analyzed using a separate Varian CP-3330 GC equipped with a thermal conductivity detector (TCD), having column dimensions of 2 m length x 2 mm diameter, with 60-80 mesh HayeSep packing and Ar as a carrier gas. Because of the close retention times of CO and CO<sub>2</sub>, another Varian CP-3330 GC was used but operated at different chromatographic conditions. The product liquid consisting of product water and bio-oil was collected in the condensers. The liquid sample was dried via a sodium sulphate packed column to remove water and the bio-oil was analyzed using a Varian CP3800 gas chromatograph coupled to a Varian Saturn 2200 GC-MS instrument equipped with DB-5 capillary column of 30 m long x 0.25 $\mu$ m.

Catalyst characterization included powder X-ray diffraction (XRD) using a Bruker D8 powder X ray diffractometer, with CuK $\alpha$  radiation at 40 kV and 40 mA. The average crystal size of the active metal particles on the catalysts was determined from XRD data using the Debye-Scherrer equation [15]. The used catalysts were also analysed by temperature-programmed oxidation (TPO) with a Shimadzu TGA 50 to determine the characteristics of any carbon deposited on the surface of catalyst. The used catalyst was heated from room temperature to 800 °C in air with a heating rate of 15 °C min<sup>-1</sup> and a holding time of 10 min at 800 °C.

### 3.0 Results and Discussion

#### 3.1. Pyrolysis-catalytic hydrogenation of cellulose, hemicellulose and lignin.

The pyrolysis-catalytic hydrogenation of cellulose, hemicellulose (xylan) and lignin was performed in the two-stage fixed bed reactor in the presence of the 10 wt.% Ni/Al<sub>2</sub>O<sub>3</sub> catalyst. The product yield and volumetric gas composition are presented in Table 3 and the gas yield in terms of mmol of gas g<sup>-1</sup><sub>biomass</sub> is presented in Figure 2. Also shown are blank experiments, where quartz sand was substituted for the catalyst. Pyrolysis took place at a heating rate of 20 °C min<sup>-1</sup> to a final temperature of 800 °C. The temperature of the catalyst was 500 °C and the hydrogen input flow rate was maintained at 3600 ml h<sup>-1</sup> g<sup>-1</sup> catalyst. Since pyrolysis was carried out in the 1<sup>st</sup> stage of the reactor at the same experimental conditions, therefore the char residue was the same for each of the biomass components irrespective of whether sand or catalyst was used in the 2<sup>nd</sup> stage. Table 3 shows that the highest char residue was observed with lignin at 39 wt.% followed by hemicellulose at 17 wt.% and cellulose at 13 wt.%. Higher char residue yield with lignin compared to hemicellulose and cellulose has been reported by other researchers [19-21]. The introduction of the 10 wt.% Ni/Al<sub>2</sub>O<sub>3</sub> catalyst to the hydrogenation process produced an increase in gas yield compared to the blank sand experiments, particularly for the hemicellulose and cellulose, but only slightly for the lignin. In the presence of the catalyst the liquid yield (oil and water) was increased for all of the biopolymers. Table 3 also shows the carbon distribution between the solid and gaseous products to produce a carbon balance. Quantitative analysis of the bio-oil proved too difficult due to the excessive product water produced and the losses of the bio-oil in the condenser transfer lines and therefore the contribution to the carbon balance could not be obtained. Table 3 shows that in the presence of

the catalyst, the gaseous yield increased significantly in the case of hemicellulose and cellulose while only a small change in the gas yield was observed with the lignin feedstock. The highest carbon distribution to the char was shown by lignin at 51.13 % followed by hemicellulose and cellulose at 35.27 % and 24.57 % respectively. Table 3 also shows that the CH<sub>4</sub>/CO and CH<sub>4</sub>/CO<sub>2</sub> ratios increased in the presence of the 10 wt.% Ni/Al<sub>2</sub>O<sub>3</sub> catalyst which indicates the promotion of the methanation reaction via producing increased yield of methane compared to the carbon oxides. The catalytic hydrogenation of the carbon oxides was also reflected in the relative gas volumetric concentrations shown in Table 3, where CH<sub>4</sub> volumetric yields were markedly increased with a consequent reduction in CO and CO<sub>2</sub> volumetric concentrations.

Figure 2 presents the individual gas yields in mmoles g<sup>-1</sup><sub>biomass</sub> and shows that the addition of the 10 wt.% Ni/Al<sub>2</sub>O<sub>3</sub> catalyst increased the methane yield from 2.3 mmoles g<sup>-1</sup><sub>biomass</sub> to 3.7 mmoles g<sup>-1</sup><sub>biomass</sub> for the lignin. However, for the hemicellulose and cellulose the increase in methane yield in the presence of the catalyst was more pronounced, increasing from ~1 mmoles g<sup>-1</sup><sub>biomass</sub> to 7.9 mmoles g<sup>-1</sup><sub>biomass</sub> and 7.65 mmoles g<sup>-1</sup><sub>biomass</sub> respectively. The high CH<sub>4</sub> yield was also reflected in the reduced yield of CO and CO<sub>2</sub>, confirming the catalytic hydrogenation of the carbon oxide gases.

The condensed liquid consisted of mainly water which is the by-product of the methanation reaction with only a small quantity of bio-oil. Qualitative analysis of the bio-oil obtained from the pyrolysis-catalytic hydrogenation of biomass components was carried out using gas chromatography-mass spectrometry. The pyrolysis-catalytic hydrogenation of cellulose and hemicellulose produced an oil containing mainly phenol and phenol derivatives and lower concentrations of other oxygenated aromatic compounds. The main product derived from the pyrolysis-catalytic hydrogenation of lignin was a complex mixture of oxygenated aromatic compounds, including phenol, alkylated phenolic compounds and dibenzofuran molecular weight. Stefanidis et al., [22] performed the pyrolysis of cellulose, hemicellulose

and lignin using ZSM-5 as the catalyst. They also reported the formation of phenol from thermal pyrolysis of cellulose and hemicellulose. Similarly, they reported the formation of complex phenolic (phenol with methoxy group) and benzenediols from the thermal pyrolysis of lignin.

Analysis of the catalyst was carried out after the pyrolysis-catalytic hydrogenation of the different biomass components using X-ray diffraction to determine any sintering of the metal particles by comparing the particle size of reacted and fresh 10 wt.% Ni/Al<sub>2</sub>O<sub>3</sub> catalysts. Results of the XRD analysis are shown in Figure 3. There was negligible change in the particle size seen after the catalytic hydrogenation of various biomass components. The Ni particle size of the fresh 10 wt.% Ni/Al<sub>2</sub>O<sub>3</sub> catalyst was calculated as 8.3 nm, while the particle size of the reacted catalyst observed from the pyrolysis-catalytic hydrogenation of cellulose, hemicellulose and lignin was 8.2, 7.1 and 9.1 nm respectively. Therefore, it can be concluded that the catalyst was stable and no-sintering of the catalyst took place during the catalytic hydrogenation process under the experimental conditions used here. Temperature programmed oxidation of the used 10 wt.% Ni/Al<sub>2</sub>O<sub>3</sub> catalysts was carried out to determine the weight loss data of the reacted catalyst to identify any carbon deposition on the catalyst. The results showed that there was negligible carbon deposited on the catalyst suggesting that any produced carbon on the catalyst reacted with input hydrogen during the catalytic hydrogenation process and produced methane.

### **3.2 Pyrolysis-catalytic hydrogenation of biopolymer mixtures**

To determine any interaction between lignin, hemicellulose and cellulose, the pyrolysis-catalytic hydrogenation of mixtures of the three biopolymers was undertaken. Hemicellulose consists of different branched saccharides and random amorphous structure facilitating

decomposition at lower temperature. The cellulose structure does not contain branched glucose structures instead it has a well ordered linear glucose-based structure contains the structure with good thermal stability. While lignin has an aromatic structure with various branches and strong chemical bonding and therefore decomposes over a wide temperature range [23]. Therefore, mixtures were based on changes in the content of lignin in the mixtures, ranging from 100, 60, 40 and wt.% lignin with a balance made-up of equal quantities of cellulose and hemicellulose. Initial experiments examined the thermal decomposition (pyrolysis) of the different mixtures using thermogravimetric analysis. Thermogravimetric analysis of the different biomass component mixtures is shown in Figure 4(a). It can be observed that the highest weight loss was obtained with the lowest percentage of lignin in the component mixture. When 100 wt.% lignin was used, the maximum weight loss percentage obtained was around 40 % but when lignin was present in the mixture at 20 wt.% and the balance was hemicellulose and cellulose, the total weight loss increased to around 22 %. It is also evident that the lignin continues to decompose over a wider temperature range and a sharp increase in weight loss was observed at around 270 °C. However, with the introduction of cellulose and hemicellulose to the lignin, a sharp decline in the weight loss peak was observed at around 220 °C. The TGA/DTG thermograms of pure cellulose, hemicellulose and lignin have been reported and discussed in the literature and differences have been attributed to differences in degradation behaviour of the different biomass components due to the differences in chemical structure [13, 24]. But, for ease of comparison with the biomass component mixtures in Figure 4, the TGA and DTG results for the individual, cellulose, hemicellulose and lignin are shown here in Figure SI 1(a) and SI 1(b) in the Supplementary Information. Figure SI 1(a) and SI 1(b) thermograms show that the initiation of decomposition of hemicellulose starts at a temperature of 210 °C with the maximum weight loss in the temperature range of 220 °C — 380 °C. Cellulose starts to decompose at ~270 °C and maximum weight loss in the temperature range

between 280 °C — 440 °C. Lignin however decomposed over a wide temperature range with maximum weight loss observed in the temperature range of 250 — 500 °C.

Figure 4(b) shows the DTG thermograms for the different mixtures of lignin and cellulose/hemicellulose. The DTG thermograms show 3 distinct peaks, two peaks (1<sup>st</sup> and 2<sup>nd</sup> peaks) below 327 °C which corresponds to the hemicellulose weight loss while the peak above 327 °C corresponds to the cellulose and some lignin weight loss. DTG analysis shows that with the increase of cellulose and hemicellulose in the mixture the 3<sup>rd</sup> DTG peak (above 327 °C) shifted towards a lower temperature of decomposition while the 1<sup>st</sup> and 2<sup>nd</sup> DTG peaks (below 327 °C) shifted slightly towards higher temperature of decomposition showing the interaction between the biomass components. According to Liu et al., [24] changes in thermal decomposition for biomass decomposition as determined by TGA/DTG that appear below 327 °C are because of the interaction of lignin with hemicellulose while changes in TGA/DTG thermograms above 327 °C are mainly because of interaction of hemicellulose with cellulose and to a lesser extent hemicellulose with lignin. The interaction of lignin, hemicellulose and cellulose using TGA/DTG systems has also been reported by other researchers [25-27]. For example, Worasuwannarak et al., [26] reported significant interaction between biomass components during pyrolysis, suggesting that interaction between cellulose and lignin increased the char yield and decreased tar yield. Yu et al., [27] studied the interaction between biomass components by comparing the predicted results from the data obtained from the individual biomass components. They reported no significant difference was observed in the case of a cellulose-lignin blend. But, when they studied the pyrolysis of three biomass components together, an increase in char yield was observed as compared to that of the predicted values. Burhenne et al., [25] used TGA and a fixed bed reactor with different biomass components and reported that lignin is an important factor in relation to product yield and gas composition.

To verify the effect of lignin content on the mixtures of cellulose/hemicellulose with lignin from the pyrolysis catalytic hydrogenation process for methane production, experiments were undertaken using the two-stage pyrolysis-catalytic hydrogenation reactor system. The percentage content of lignin in the mixture was the same as that used with the TGA experiments, i.e. 100 wt.%, 60 wt.%, 40 wt.% and 20 wt.% lignin with the balance made up of an equal mass of cellulose and hemicellulose. All the experiments were conducted in the presence of the 10 wt.% Ni/Al<sub>2</sub>O<sub>3</sub> catalyst with a final 1<sup>st</sup> stage pyrolysis temperature of 800 °C and catalytic hydrogenation temperature of 500 °C. The H<sub>2</sub> space velocity was kept constant at 3600 ml h<sup>-1</sup> g<sup>-1</sup> catalyst. The product yield and gas compositions are shown in Table 4. The results show that the char residue yield decreased from 39 wt.% to 22 wt.% with the decrease in lignin content in the component mixture. There was a corresponding increase in liquid yield from 17 wt.% to 35 wt.% and increase in gas yield from 45.8 wt.% to 59.8 wt.% with the decrease in lignin content. The distribution of carbon between solid and gaseous products was determined by calculating a carbon balance and the results are shown in Table 4. It can be seen from Table 4 that with the decrease of percentage lignin in the mixture from 60 wt.% to 20 wt.% in the bi-polymer mixtures, the percentage of carbon in the gas fraction increased significantly from 13.19 % to 29.64 % showing the conversion of higher molecular weight hydrocarbons into lower molecular weight gaseous hydrocarbons. Also, the distribution of carbon in the char reduced from 51.13 % to 34.66 % with the decrease of lignin and increase in cellulose and hemicellulose in the bi-polymer mixture composition.

The results from the TGA/DTG experiments with the different biopolymer mixtures reported earlier, suggested some interaction of the components with shifts in the temperature of decomposition for the hemicellulose and cellulose components in particular. Figure 5 shows the individual gas composition in mmol g<sup>-1</sup><sub>biomass</sub> in relation to the decrease in lignin content in

the biopolymer component mixtures from 100 wt.% to 20 wt.%. It can be observed that the methane yield increased from 3.73 mmol g<sup>-1</sup><sub>biomass</sub> with the 100 wt.% lignin to significantly higher yields of methane when hemicellulose and cellulose were added to the biopolymer mixture, linked to the promotion of reforming and methanation reactions. The results of the pyrolysis-catalytic hydrogenation of the lignin with hemicellulose/cellulose mixtures shown in Table 4 and Figure 5 exhibited a synergistic interaction of the biopolymers. Figure 6 shows the total gas yield and the methane yield in the form of a comparison of the calculated and experimental results for the pyrolysis-catalytic hydrogenation of biomass components with different lignin percentage in the mixture. The calculated data were based on the total gas yields and methane yields obtained from the pyrolysis-catalytic hydrogenation of the individual lignin, hemicellulose and cellulose and their relative compositions in the biopolymer mixture. Figure 6 shows that the experimentally determined total gas yield and methane yield in terms of mmol CH<sub>4</sub> g<sup>-1</sup><sub>biomass</sub> were significantly higher compared to the expected values calculated from the pyrolysis-catalytic hydrogenation of the individual biopolymers shown in Table 3 and Figure 2. For example, the calculated methane yield values as mmol CH<sub>4</sub> g<sup>-1</sup><sub>biomass</sub> for 60 wt.%, 40 wt.% and 20 wt.% lignin content were 5.35, 6.15 and 6.96 mmol CH<sub>4</sub> g<sup>-1</sup><sub>biomass</sub> respectively. However, the experimentally obtained methane yield values at 60 wt.%, 40 wt.% and 20 wt.% lignin content were significantly higher at 6.80, 6.84 and 7.36 mmol g<sup>-1</sup><sub>biomass</sub> respectively.

### **3.3 Product yield from the catalytic hydrogenation of agricultural biomass waste.**

The pyrolysis-catalytic hydrogenation of the four agricultural waste biomass samples was undertaken to determine their methane yields. However, initial work was carried out to determine their thermal degradation profiles using TGA. The TGA and DTG thermograms of the different agricultural waste biomass types used in this work are shown in Figure 7. It can

be observed from the TGA decomposition behavior that agricultural waste biomasses decompose in the range of decomposition temperatures shown by the biomass components. The decomposition of the agricultural waste samples may be linked to the decomposition of the biomass components of the biomass [17]. For example, the DTG thermograms of some agricultural waste biomasses exhibited more than one peak which indicates the presence of the biomass components, cellulose, hemicellulose and lignin in the waste biomass. The composition of a wide range of biomass types in relation to the various proportions of cellulose, hemicellulose and lignin have been reported in the literature. For example, it has been reported that sugarcane bagasse on average contains 23-32 wt.% of lignin and 19-24 wt.% of cellulose and 32-48 wt.% hemicellulose. Willow contains around 20 wt.% of lignin and 49 wt.% of cellulose and 14 wt.% of hemicellulose. While rice straw has been reported to contain 18 wt.% of lignin, 32 wt.% cellulose and 24 wt.% of hemicellulose [28-30]. No data on the biopolymer composition of ugu plant could be found in the literature.

The DTG thermograms of the agricultural waste biomasses show that the highest weight loss peak was observed with the willow and sugar cane bagasse in the temperature range of 350 – 400 °C which is linked to the presence of a higher percentage of cellulose compared to that of ugu plant and rice straw. Varhegyi et al., [31] studied the thermal decomposition behavior of sugar cane bagasse using TGA and also observed three thermal degradation peaks. They suggested that the first two peaks were attributed to the presence of hemicellulose while the third peak was attributed to the presence of cellulose. Bridgeman et al., [29] reported that willow contains a high percentage of cellulose and lignin and lower quantities of hemicellulose. Similarly, in our results, one single large DTG peak was observed in the range of 350-400 °C attributed to the presence of more cellulose as compared to that of hemicellulose. In the case of rice straw and ugu plant biomasses, thermal degradation starts at a lower temperature compared to that of willow. Which suggests the presence of some hemicellulose in the biomass.

However, the maximum peak was observed at 300-400 °C showing the overlapping of hemicellulose and cellulose thermal degradation. Huang et al., [32] performed TGA of rice straw and stated that cellulose is the main component of rice straw. Since ugu plant showed almost the same behavior to that of rice straw it can be suggested that cellulose is also the main component of ugu plant.

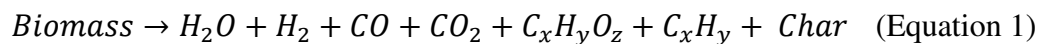
The pyrolysis-catalytic hydrogenation of agricultural waste biomass was performed in the two-stage fixed bed reactor and the results of product yield and gas composition are shown in Table 5. The experiments were performed using 10 wt.% Ni/Al<sub>2</sub>O<sub>3</sub> catalyst in the 2<sup>nd</sup> stage of the reactor with a catalytic hydrogenation temperature at 500 °C and a final pyrolysis temperature of 800 °C. The results show that the highest char yield was produced by rice straw at 28 wt.% while the lowest char yield was produced by willow and sugar cane bagasse at 23 wt.%. The highest liquid yield was obtained with sugarcane bagasse at 32 wt.% and the lowest was shown by rice straw at 18 wt.%. This is in agreement with the TGA and DTG thermograms shown in Figure 7. As shown in Table 5 the maximum CH<sub>4</sub>/CO ratio was shown by ugu plant which can be attributed to the limited formation of CO from biomass. The differences in volumetric methane gas composition for the different biomass samples was similar at ~70 vol.% of CH<sub>4</sub>.

Figure 8 shows the gas yield in terms mmol g<sup>-1</sup> biomass from the agricultural biomass samples. The highest methane yield was shown by willow at 8.87 mmol g<sup>-1</sup> biomass. Methane yield decreased in the following order willow > sugarcane bagasse > ugu plant > rice straw. Also, the highest CO<sub>2</sub> and CO at 2.2 mmol g<sup>-1</sup> biomass and 1.7 mmol g<sup>-1</sup> biomass was shown by willow. These results are linked with the TGA and DTG data and physio-chemical properties reported in Table 1 and Table 2, suggesting that the composition of willow and sugarcane bagasse are similar while rice straw and ugu plant are different from the other two biomasses. In particular, the higher volatile content of willow and sugarcane bagasse suggests a high

content of hemicellulose and lignin, as also suggested by the TGA/DTG results. Figure 2 shows that a hemicellulose and cellulose produce significantly higher yields of methane compared to lignin. Therefore, the higher yield of methane from willow and sugarcane bagasse is indicative of a higher hemicellulose and cellulose content of these two biomass types.

### 3.4 Reaction Mechanism

The various mechanistic steps involved in the overall process of biomass pyrolysis, thermal cracking and catalytic hydrogenation have been proposed separately by several authors [33-38]. The mechanism of pyrolysis of biomass by thermal degradation of biomass into solid biochar, bio-oil and gaseous products via pyrolysis is shown in equation 1 [33]. The evolved bio-oil vapours and pyrolysis gases from the 1<sup>st</sup> stage pyrolysis reactor enters the catalytic reactor in the presence of added hydrogen and undergoes thermal cracking to convert the higher hydrocarbons into H<sub>2</sub>, lower hydrocarbons including CH<sub>4</sub> and carbon oxides (Equation 2). The CO<sub>2</sub> and CO derived directly from biomass pyrolysis and also from thermal cracking reactions of the pyrolysis vapours are catalytically hydrogenated with the added hydrogen to produce CH<sub>4</sub> (equations 3 and 4).



It has been reported that during CO<sub>2</sub> and CO disassociation over the catalyst, oxygenated species are formed as intermediate products. In the literature it has been reported that during CO dissociation over Ni/Al<sub>2</sub>O<sub>3</sub> catalyst a methoxy group is formed as an intermediate product. According to Pan et al., [34] oxygenated intermediates are formed during

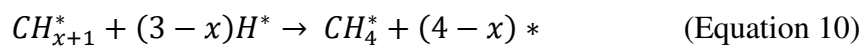
CO<sub>2</sub> disassociation. They reported the formation of intermediate carbonate and formate over the basic sites of the catalyst. During the methanation process, H<sub>2</sub> is activated over Ni species, suggested from previous studies performed by Garbarino et al [35] who carried out the methanation reaction over non-reduced Ni catalysts. They also observed inactivity of the catalyst with the non-reduced catalyst [35]. But for the conversion of CO<sub>2</sub> to methane, the interaction of a metal with the support is required or the size of the metal particle should be sufficiently high. According to Garbarino et al., [35] a strong interaction between Ni and support is required to convert CO<sub>2</sub> directly or indirectly (intermediate CO formation) into methane. This avoids the desorption of the carbon oxides. The detailed methanation reaction mechanism is reported to involve three reaction steps, adsorption, surface reaction and desorption (Equations 5 – 14). The first step includes the adsorption of reactant gases on the active sites of the catalytic surface. In this process, adsorption of CO and dissociative adsorption of hydrogen and CO<sub>2</sub> takes place and results in the formation of hydrogen atoms, adsorbed CO and oxygen atoms (eqs. 5 - 7). Some studies have proposed that the CO<sub>2</sub> methanation reaction proceeds without dissociation of CO<sub>2</sub> into CO<sub>ads</sub> [36]. While Eckle et al., [37] studied the intermediate and side products formation during the CO<sub>2</sub> methanation reaction and reported that the CO<sub>2</sub> methanation reaction takes place via CO<sub>2</sub> dissociation to CO<sub>ads</sub>. They suggested that the formation and decomposition of formate species, produced during the direct conversion of CO<sub>2</sub> to methane, plays a very minor role in CO<sub>2</sub> methanation. The second step involves surface reactions where adsorbed CO reacts with atomic hydrogen to undergo methanation. There are some studies which suggest that the direct dissociation of CO into CH<sub>x</sub> without the formation of any hydrogen assisted intermediates. While Ojeda et al., [38] provided the theoretical and experimental evidence for CO dissociation through hydrogen assisted intermediates into methane. They proposed that hydrogen assisted CO dissociation is more feasible because of the relatively lower activation energy barrier as compared to unassisted CO

dissociation.  $\text{HCO}_{\text{ad}}$  was observed as an intermediate product during CO methanation reaction (eq. 8). Functional groups ( $\text{HCO}_{\text{ad}}$ ) continue to combine with hydrogen atoms to release oxygen atoms and ultimately results in the formation of  $\text{CH}_x$  (eq. 9). Water formation during the methanation reaction is irreversible because of the relatively higher activation energy barrier of the reverse reaction. The oxygen atoms ( $\text{O}^*$ ) produced react with hydrogen atoms ( $\text{H}^*$ ) to produce  $\text{OH}^*$  and this  $\text{OH}^*$  further hydrogenates to produce water (eq. 11 and eq. 12). The third step in the detailed reaction mechanism is the desorption stage where the produced  $\text{CH}_4$  and  $\text{H}_2\text{O}$  desorbs from the catalyst surface (eq. 13) and (eq. 14) leaving behind the active sites for the remaining gases to adsorb on the catalyst surface.

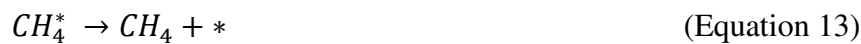
Adsorption Reaction:



Surface Reaction:



Desorption Reaction:



The results reported here show that it is possible to generate significant quantities of methane from waste biomass. Production of methane as a substitute natural gas has advantages

in that the product gas can be distributed via the already existing natural gas infrastructure and distribution facilities available in most countries [7,8]. A further advantage is that the substitute natural gas would be derived from sustainable biomass feedstock, rather than fossil fuel natural gas. The source for the hydrogen for the catalytic hydrogenation of the biomass pyrolysis gases is an issue. However, production of hydrogen from water by electrolysis using off-peak electricity generated from renewable sources such as wind, wave and solar power is a potential solution for a low cost source of hydrogen [39].

#### 4.0 Conclusions

In this study, we have reported on the influence of biomass components, cellulose, hemicellulose and lignin for the production of methane (synthetic natural gas) by a pyrolysis-catalytic hydrogenation process in a two-stage reactor. To understand the role of each component of biomass for methane production, each biomass component was studied separately and in the form of mixtures. In addition, four different agricultural waste biomasses were also studied to estimate the effect of biomass composition on methane production.

The results showed that with the addition of a 10 wt.% Ni/Al<sub>2</sub>O<sub>3</sub> catalyst, methane production was enhanced significantly compared to a baseline non-catalytic process (quartz sand substituted for the catalyst). For example, in the absence of any catalyst the highest CH<sub>4</sub> yield was produced from lignin at 2.2 mmoles g<sup>-1</sup><sub>biomass</sub> and with hemicellulose and cellulose the CH<sub>4</sub> yield was ~1 mmoles g<sup>-1</sup><sub>biomass</sub>. However, with the addition of the 10 wt.% Ni/Al<sub>2</sub>O<sub>3</sub> catalyst, the CH<sub>4</sub> yield for lignin increased to 3.7 mmoles g<sup>-1</sup><sub>biomass</sub>, but markedly higher methane yields were obtained for hemicellulose (7.9 mmoles g<sup>-1</sup><sub>biomass</sub>) and cellulose (7.65 mmoles g<sup>-1</sup><sub>biomass</sub>).

The pyrolysis-catalytic hydrogenation of different mixtures of the biomass components showed that the presence of hemicellulose and cellulose were the main controlling factor in terms of methane gas yield, since these two components produced significantly more methane than lignin. Experiments using mixtures of lignin with hemicellulose/cellulose with different lignin contents using TGA showed interaction between the components with a shift in the thermal decomposition temperature for both hemicellulose and cellulose. The interaction between biomass components using TGA was also observed for the pyrolysis-catalytic hydrogenation experiments in the two-stage reactor system. The total gas yield and also the methane yield showed a significant increase for the experimental values compared to the calculated yields based on the pyrolysis-catalytic hydrogenation of the individual biopolymers. For the pyrolysis catalytic hydrogenation of agricultural waste biomass, the highest methane yield was observed with the willow and sugarcane bagasse while the minimum was observed with rice straw. The higher yield of methane from willow and sugarcane bagasse was linked to the higher content of hemicellulose and cellulose in these two biomasses.

**References:**

- [1]. Sharma, H.K., C. Xu and W. Qin, Biological pretreatment of lignocellulosic biomass for biofuels and bioproducts: An overview. *Waste and Biomass Valorization*, 2019. 10(2): 235-251.
- [2]. Sanna, A., Advanced Biofuels from Thermochemical processing of sustainable biomass in Europe. *BioEnergy Research*, 2014. 7(1): 36-47.
- [3]. Tripathi, M., J.N. Sahu and P. Ganesan, Effect of process parameters on production of biochar from biomass waste through pyrolysis: A review. *Renewable and Sustainable Energy Reviews*, 2016. 55: 467-481.
- [4]. Weiland, P., Biogas production: current state and perspectives. *Applied Microbiology and Biotechnology*, 2010. 85(4): 849-860.
- [5]. Yang, H., R. Yan, H. Chen, D.H. Lee, and C. Zheng, Characteristics of hemicellulose, cellulose and lignin pyrolysis. *Fuel*, 2007. 86(12): 1781-1788.
- [6]. Uzi, A., Y. Shen, S. Kawi, A. Levy, and C.-H. Wang, Permittivity and chemical characterization of woody biomass during pyrolysis and gasification. *Chemical Engineering Journal*, 2019. 355: 255-268.
- [7]. Ogden, J., A.M. Jaffe, D. Scheitrum, Z. McDonald, and M. Miller, Natural gas as a bridge to hydrogen transportation fuel: Insights from the literature. *Energy Policy*, 2018. 115: 317-329.
- [8]. Keefer, B.G., M.L. Babicki, B.G. Sellars, and E. Ng, Method and system for biomass hydrogasification. 2016, Google Patents.
- [9]. Janke, L., B.K. McCabe, P. Harris, A. Hill, S. Lee, S. Weinrich, S. Marchuk, and C. Baillie, Ensiling fermentation reveals pre-treatment effects for anaerobic digestion of sugarcane biomass: An assessment of ensiling additives on methane potential. *Bioresource Technology*, 2019. 279: 398-403.
- [10]. Dahunsi, S.O., Mechanical pretreatment of lignocelluloses for enhanced biogas production: Methane yield prediction from biomass structural components. *Bioresource Technology*, 2019. 280: 18-26.
- [11]. Franco, R.T., P. Buffière and R. Bayard, Co-ensiling of cattle manure before biogas production: Effects of fermentation stimulants and inhibitors on biomass and methane preservation. *Renewable Energy*, 2018. 121: 315-323.
- [12]. Mihet, M. and M.D. Lazar. Methanation of CO<sub>2</sub> on Ni/ $\gamma$ -Al<sub>2</sub>O<sub>3</sub>: Influence of Pt, Pd or Rh promotion. *Catalysis Today*, 2018, 306, 294-299.
- [13]. Du, G., S. Lim, Y. Yang, C. Wang, L. Pfefferle and G.L. Haller. Methanation of carbon dioxide on Ni-incorporated MCM-41 catalysts: The influence of catalyst pretreatment and study of steady-state reaction. *Journal of Catalysis*, 2007, 249(2), 370-379.
- [14]. Tatsumi, T., K.A. Koyano, Y. Tanaka and S. Nakata. Mechanical Stability of Mesoporous Materials, MCM-48 and MCM-41. *Journal of Porous Materials*, 1999, 6(1), 13-17.

- [15]. Jaffar, M.M., M.A. Nahil and P.T. Williams. Methane production from the pyrolysis–catalytic hydrogenation of waste biomass: Influence of process conditions and catalyst type. *Energy & Fuels*, 2019, 33(8), 7443-7457.
- [16]. Aziz, M.A.A., A.A. Jalil, S. Triwahyono and S.M. Sidik. Methanation of carbon dioxide on metal-promoted mesostructured silica nanoparticles. *Applied Catalysis A: General*, 2014, 486, 115-122.
- [17]. McKendry, P., Energy production from biomass (part 1): overview of biomass. *Bioresource Technology*, 2002. 83(1): 37-46.
- [18]. Le, T.A., J.K. Kang, S.H. Lee, and E.D. Park, CO and CO<sub>2</sub> methanation over Ni/  $\gamma$ -Al<sub>2</sub>O<sub>3</sub> prepared by deposition-precipitation method. *Journal of Nanoscience and Nanotechnology*, 2019. 19(6): 3252-3262.
- [19]. Rutkowski, P., Pyrolysis of cellulose, xylan and lignin with the K<sub>2</sub>CO<sub>3</sub> and ZnCl<sub>2</sub> addition for bio-oil production. *Fuel Processing Technology*, 2011. 92(3): 517-522.
- [20]. Wu, C., Wang Z., Huang J., Williams P.T., Pyrolysis/gasification of cellulose, hemicellulose and lignin for hydrogen production in the presence of various nickel-based catalysts. *Fuel*, 2013. 106: 697-706.
- [21]. Zhao, S., M. Liu, L. Zhao, and L. Zhu, Influence of interactions among three biomass components on the pyrolysis behavior. *Industrial & Engineering Chemistry Research*, 2018. 57(15): 5241-5249.
- [22]. Stefanidis, S.D., K.G. Kalogiannis, E.F. Iliopoulou, C.M. Michailof, P.A. Pilavachi and A.A. Lappas. A study of lignocellulosic biomass pyrolysis via the pyrolysis of cellulose, hemicellulose and lignin. *Journal of Analytical and Applied Pyrolysis*, 2014, 105, 143-150.
- [23]. Zhao, C., E. Jiang and A. Chen, Volatile production from pyrolysis of cellulose, hemicellulose and lignin. *Journal of the Energy Institute*, 2017. 90(6): 902-913.
- [24]. Liu, Q., Z. Zhong, S. Wang, and Z. Luo, Interactions of biomass components during pyrolysis: A TG-FTIR study. *Journal of Analytical and Applied Pyrolysis*, 2011. 90(2): 213-218.
- [25]. Burhenne, L., J. Messmer, T. Aicher, and M.-P. Laborie, The effect of the biomass components lignin, cellulose and hemicellulose on TGA and fixed bed pyrolysis. *Journal of Analytical and Applied Pyrolysis*, 2013. 101: 177-184.
- [26]. Worasuwannarak, N., T. Sonobe and W. Tanthapanichakoon, Pyrolysis behaviors of rice straw, rice husk, and corncob by TG-MS technique. *Journal of Analytical and Applied Pyrolysis*, 2007. 78(2): 265-271.
- [27]. Yu, J., N. Paterson, J. Blamey, and M. Millan, Cellulose, xylan and lignin interactions during pyrolysis of lignocellulosic biomass. *Fuel*, 2017. 191: 140-149.
- [28]. Abbasi, T. and S.A. Abbasi, Biomass energy and the environmental impacts associated with its production and utilization. *Renewable and Sustainable Energy Reviews*, 2010. 14(3): 919-937.

- [29]. Bridgeman, T.G., Jones J.M., Shield I., Williams P.T., Torrefaction of reed canary grass, wheat straw and willow to enhance solid fuel qualities and combustion properties. *Fuel*, 2008. 87(6): 844-856.
- [30]. Prasad, S., A. Singh and H.C. Joshi, Ethanol as an alternative fuel from agricultural, industrial and urban residues. *Resources, Conservation and Recycling*, 2007. 50(1): 1-39.
- [31]. Varhegyi, G., M.J. Antal Jr, T. Szekely, P.J.E. Szabo, and Fuels, Kinetics of the thermal decomposition of cellulose, hemicellulose, and sugarcane bagasse. 1989. 3(3): 329-335.
- [32]. Huang, Y.F., W.H. Kuan, S.L. Lo, and C.F. Lin, Hydrogen-rich fuel gas from rice straw via microwave-induced pyrolysis. *Bioresource Technology*, 2010. 101(6): 1968-1973.
- [33]. Dong L. Wu C., Ling H., Shi J., Williams P.T., Huang J. Promoting hydrogen production and minimizing catalyst deactivation from the pyrolysis-catalytic steam reforming of biomass on nanosized NiZnAlOx catalysts. *Fuel*, 188, 610-620, 2017
- [34]. Pan, Q., J. Peng, T. Sun, S. Wang, and S. Wang, Insight into the reaction route of CO<sub>2</sub> methanation: Promotion effect of medium basic sites. *Catalysis Communications*, 2014. 45: 74-78.
- [35]. Garbarino, G., P. Riani, L. Magistri, and G. Busca, A study of the methanation of carbon dioxide on Ni/Al<sub>2</sub>O<sub>3</sub> catalysts at atmospheric pressure. *International Journal of Hydrogen Energy*, 2014. 39(22): 11557-11565.
- [36]. Aldana, P.A.U., et al., Catalytic CO<sub>2</sub> valorization into CH<sub>4</sub> on Ni-based ceria-zirconia. Reaction mechanism by operando IR spectroscopy. *Catalysis Today*, 2013. 215: 201-207.
- [37]. Eckle, S., H.-G. Anfang, and R.J. Behm, Reaction intermediates and side products in the methanation of CO and CO<sub>2</sub> over supported Ru catalysts in h<sub>2</sub>-rich reformat gases. *The Journal of Physical Chemistry C*, 2011. 115(4): 1361-1367.
- [38]. Ojeda, M., Nabar R., Nilekar A.U., Ishikawa A., Mavrikakis M., Iglesia E., CO activation pathways and the mechanism of Fischer–Tropsch synthesis. *Journal of Catalysis*, 2010. 272(2): 287-297.
- [39]. Hydrogen Roadmap Europe; A sustainable pathway for the European energy transition. Fuel Cells and Hydrogen 2 Joint Undertaking, Publication of the European Union, Luxembourg, 2019

## FIGURE CAPTIONS

**Figure 1.** Schematic diagram of the two-stage fixed bed pyrolysis- catalytic hydrogenation reactor.

**Figure 2.** Gas yield from the pyrolysis-catalytic hydrogenation of cellulose, hemicellulose and lignin ( $\text{mmol g}^{-1}$  biomass)

**Figure 3.** Comparison of XRD pattern between fresh catalyst and reacted catalysts from pyrolysis-catalytic hydrogenation of cellulose, hemicellulose and lignin (catalytic bed temperature ( $500\text{ }^{\circ}\text{C}$ ))

**Figure 4.** Thermograms of mixtures of biomass components with varied lignin percentage in the mixture, (a) TGA and (b) DTG thermograms

**Figure 5.** Gas yield from the pyrolysis-catalytic hydrogenation of biomass components with different lignin percentage in the mixture

**Figure 6.** Comparison of calculated and experimental (a) total gas yield and (b) methane yield results for the pyrolysis-catalytic hydrogenation of biomass components with different lignin percentage in the mixture.

**Figure 7.** Thermograms of agricultural waste biomasses (a) TGA and (b) DTG thermograms.

**Figure 8.** Gas yield from the pyrolysis-catalytic hydrogenation of agricultural waste biomasses.

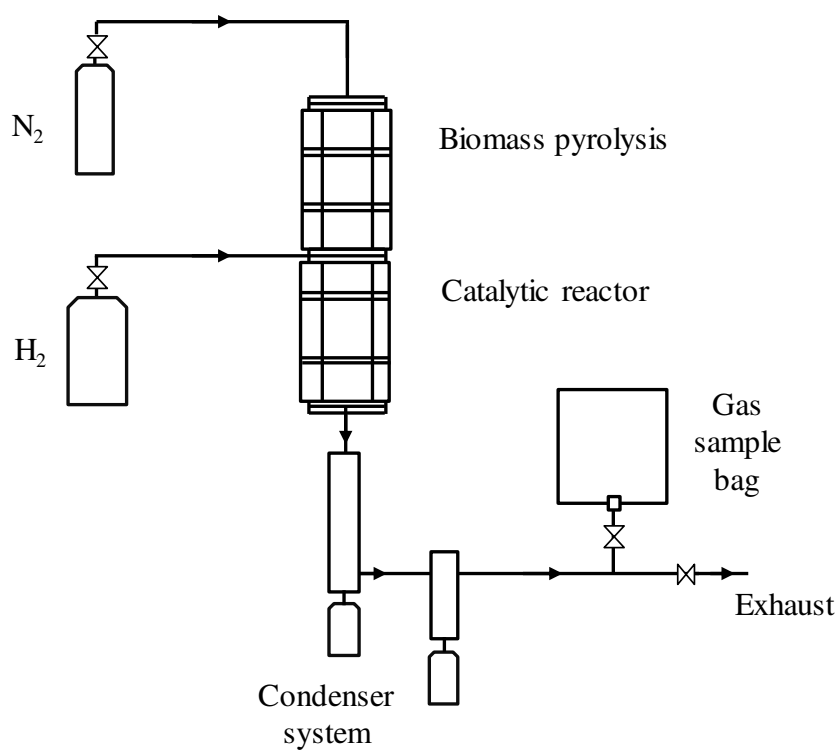


**Figure 1.** Schematic diagram of the two-stage fixed bed pyrolysis- catalytic hydrogenation reactor.

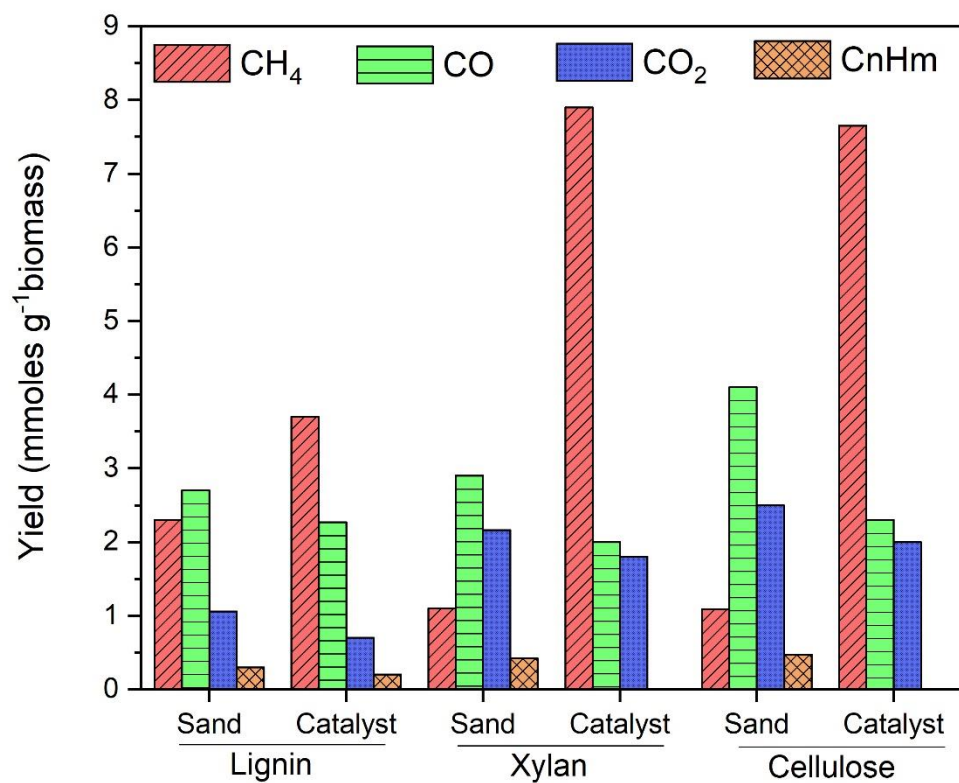


**Figure 2.** Gas yield from the pyrolysis-catalytic hydrogenation of cellulose, hemicellulose and lignin (mmol g<sup>-1</sup> biomass).

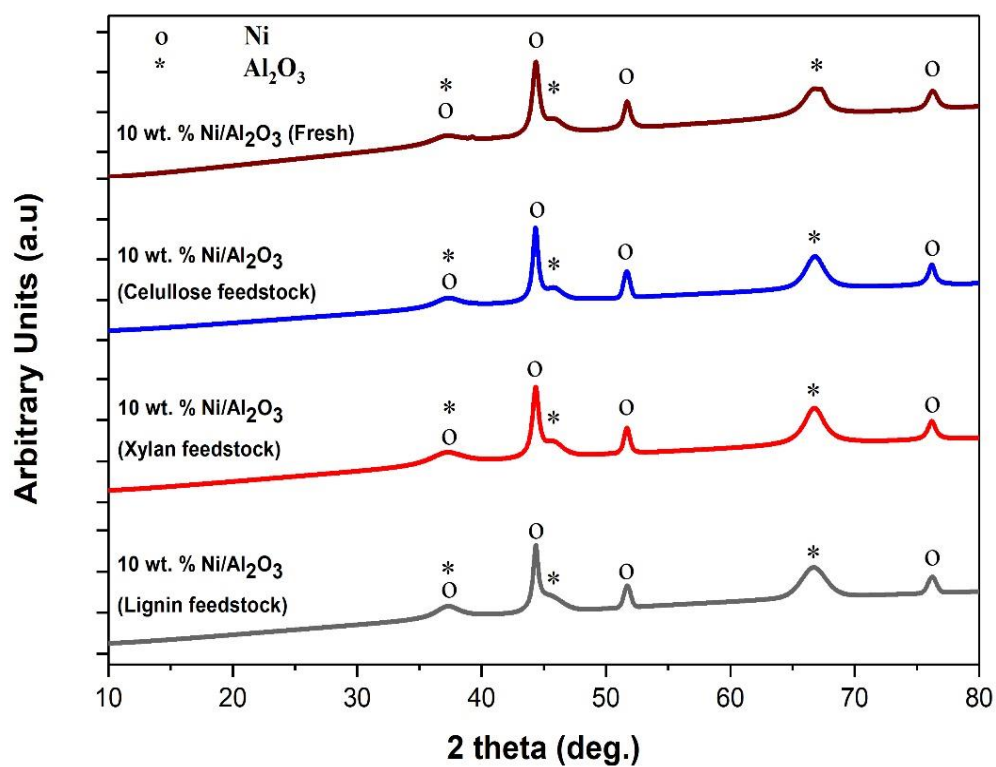


**Figure 3.** Comparison of XRD pattern between fresh catalyst and reacted catalysts from pyrolysis-catalytic hydrogenation of cellulose, hemicellulose and lignin (catalytic bed temperature (500 °C)).

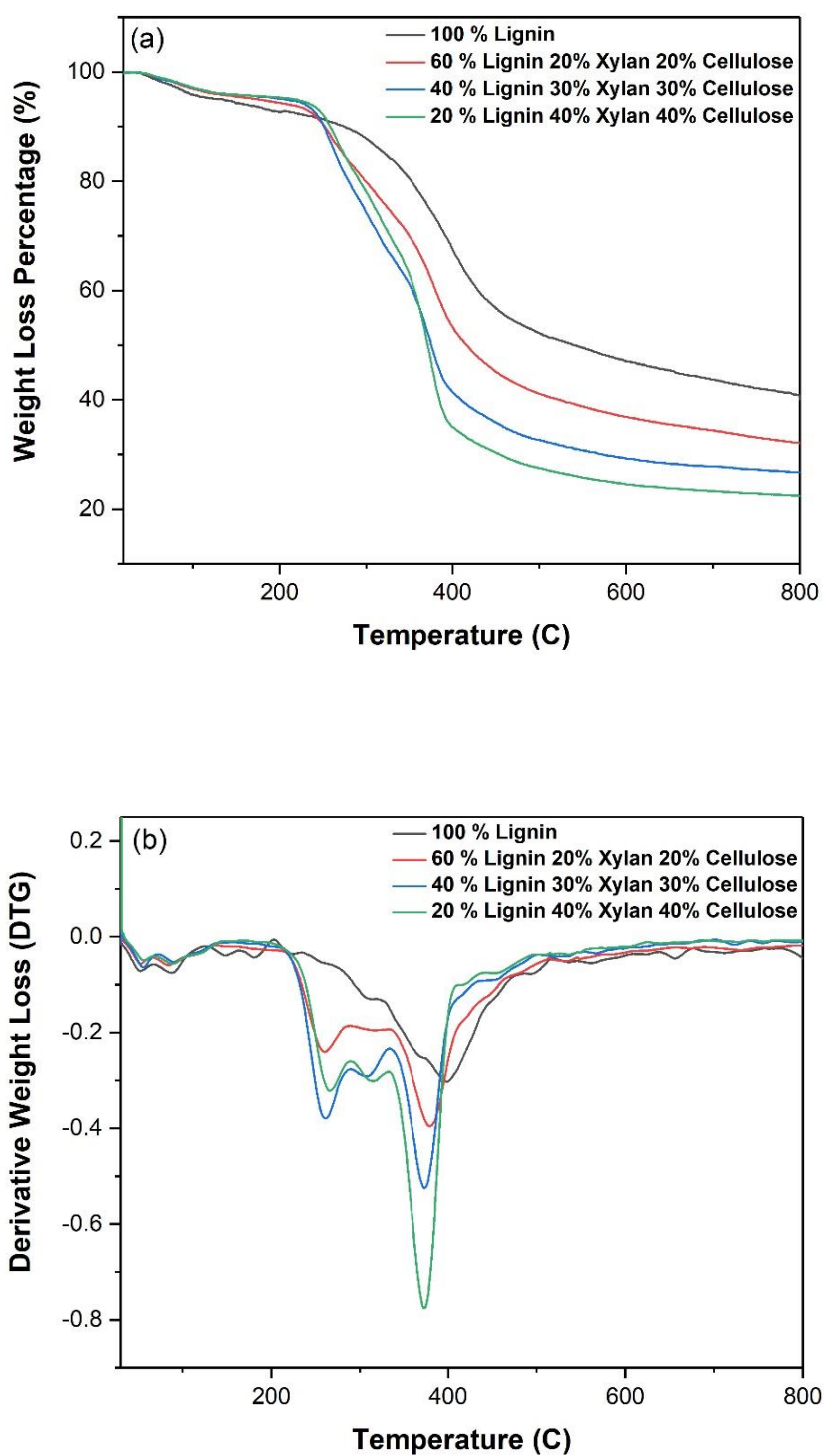


**Figure 4.** Thermograms of mixtures of biomass components with varied lignin percentage in the mixture, (a) TGA and (b) DTG thermograms

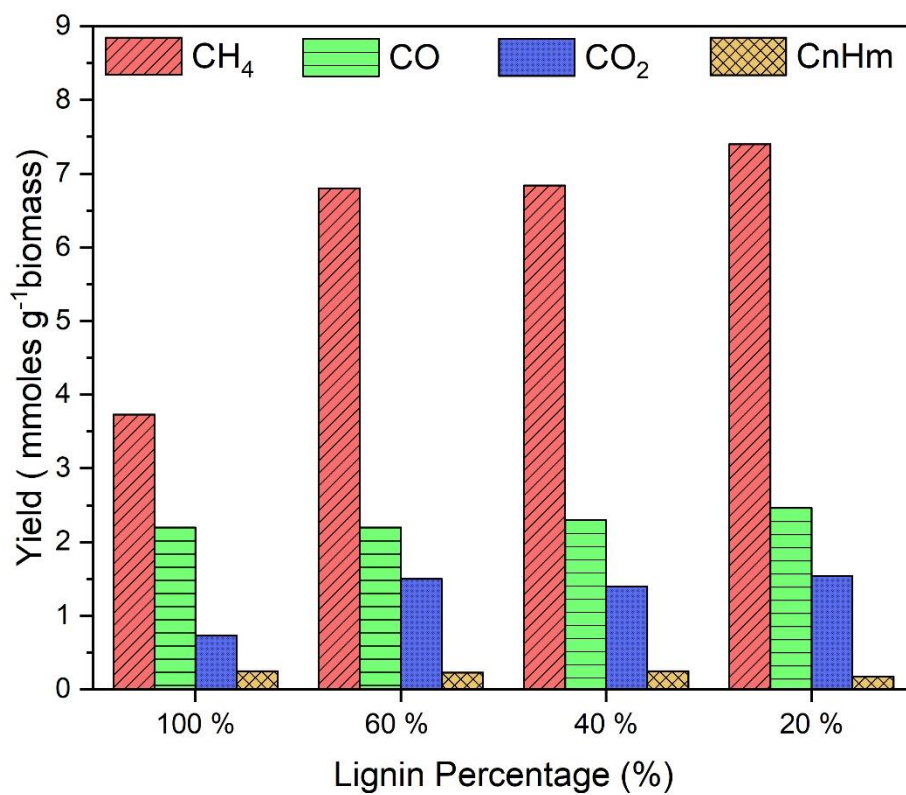


**Figure 5.** Gas yield from the pyrolysis-catalytic hydrogenation of biomass components with different lignin percentage in the mixture.

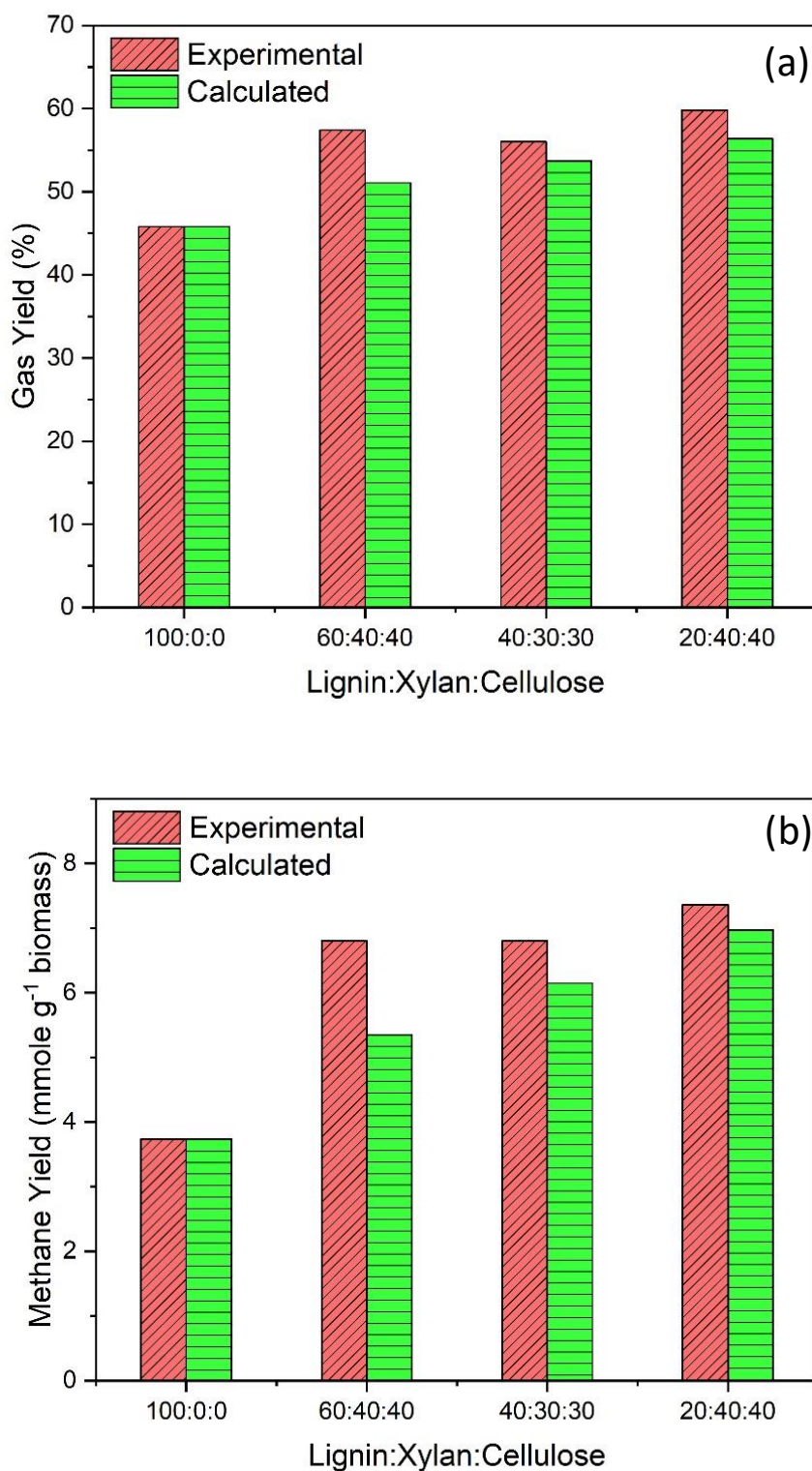


**Figure 6.** Comparison of calculated and experimental (a) total gas yield and (b) methane yield results for the pyrolysis-catalytic hydrogenation of biomass components with different lignin percentage in the mixture.

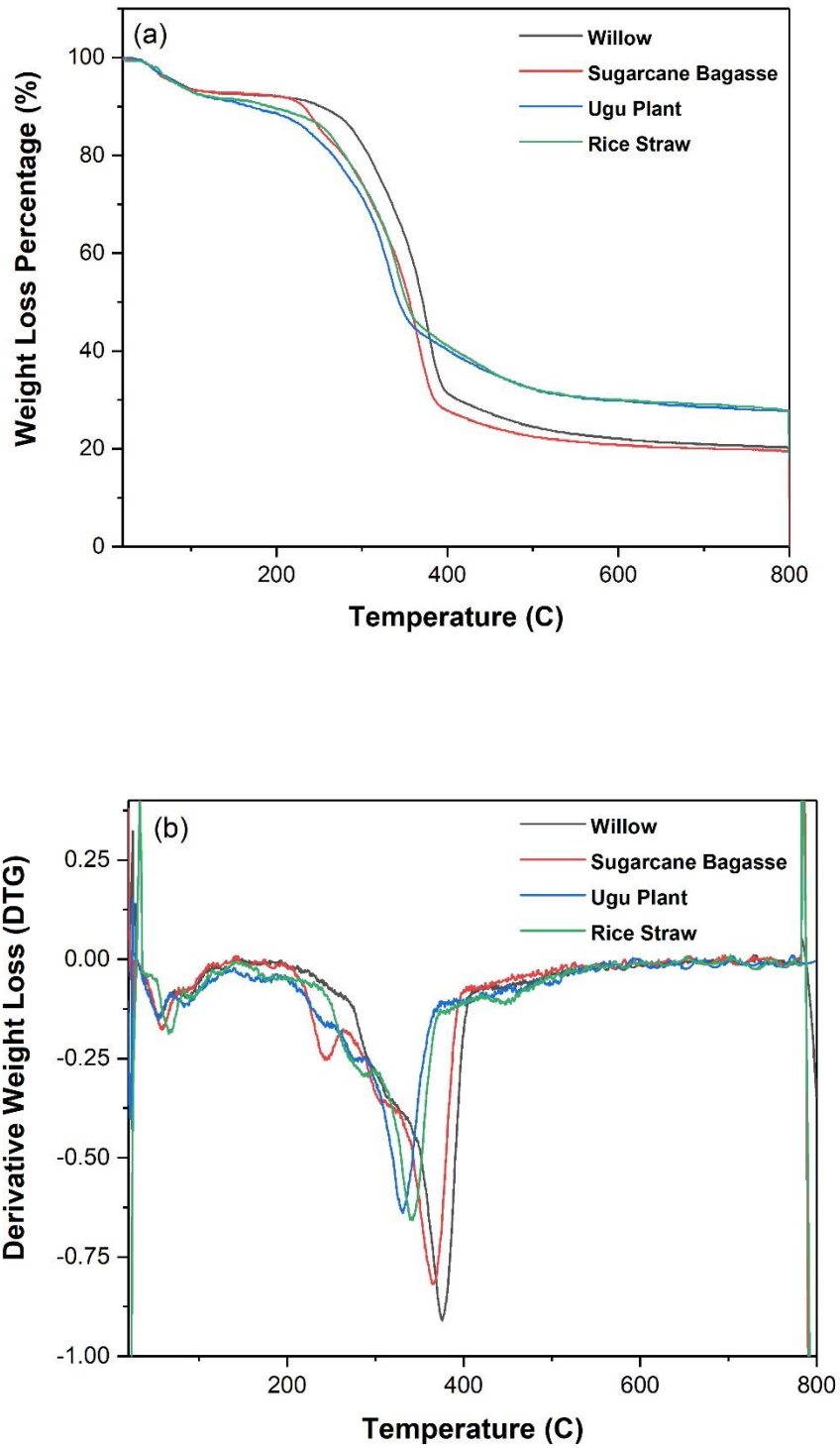


**Figure 7.** Thermograms of agricultural waste biomasses (a) TGA and (b) DTG thermograms.

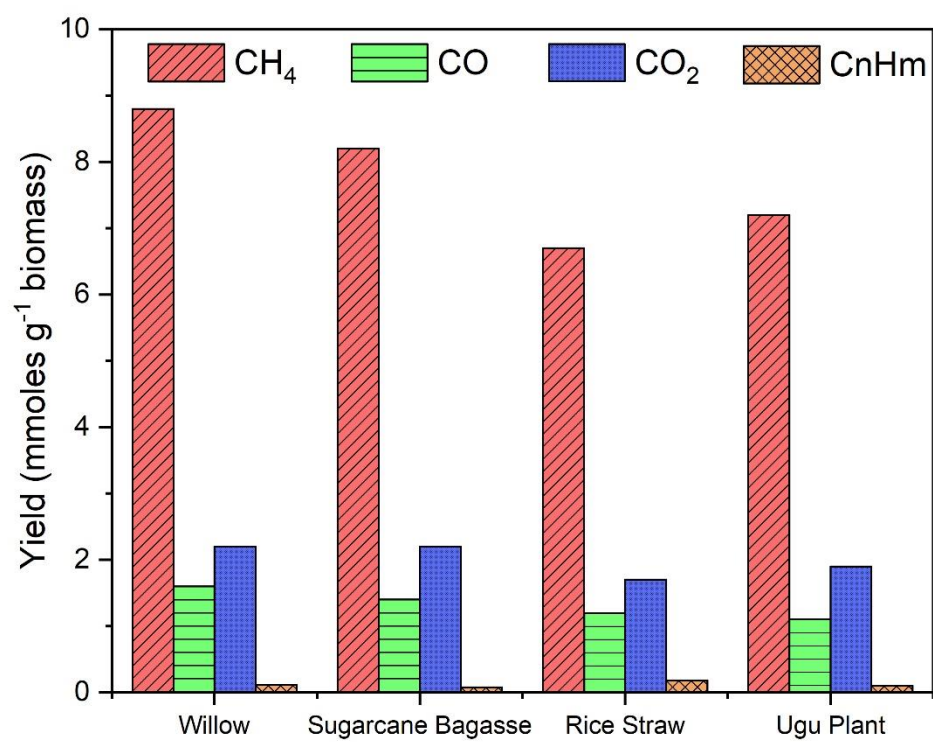


**Figure 8.** Gas yield from the pyrolysis-catalytic hydrogenation of agricultural waste biomasses.

**Table 1.** Elemental analysis of the biomass components and agricultural waste biomass.

<b>Sample</b>	<b>C</b> (wt.%)	<b>H</b> (wt.%)	<b>N</b> (wt.%)	<b>O</b> (wt.%)	<b>S</b> (wt.%)	<b>GCV</b> (k Cal. kg <sup>-1</sup> )	<b>NCV</b> (k Cal. kg <sup>-1</sup> )
Cellulose	43.26	6.41	0.29	50.04	0.00	5751	5422
Hemicellulose	43.12	6.70	0.31	49.87	0.00	5840	5496
Lignin	61.16	5.14	1.22	31.05	1.43	6819	6555
Willow	46.86	5.77	0.75	46.62	0.00	5827	5531
Rice straw	39.97	5.35	2.76	51.92	0.00	5118	4843
Ugu Plant	39.99	5.33	3.53	51.15	0.00	5113	4839
Bagasse	44.00	5.60	0.56	49.84	0.00	5534	5246

**Table 2.** Properties of the biomass components and agricultural waste biomass determined by TGA.

<b>Sample</b>	<b>Moisture (wt.%)</b>	<b>Volatiles (wt.%)</b>	<b>Fixed Carbon (wt.%)</b>	<b>Ash (wt.%)</b>
Cellulose	4.7	84.2	9.8	1.3
Xylan	3.3	82.2	12.1	2.3
Lignin	3.4	57.5	34.1	5.0
Willow	6.6	84.4	7.0	2.0
Bagasse	6.1	88.0	4.3	1.6
Rice straw	7.8	71.3	16.3	4.6
Ugu Plant	8.3	68.1	18.2	5.4

**Table 3.** Product yield and volumetric gas composition of the gases from pyrolysis-catalytic hydrogenation of cellulose, hemicellulose and lignin.

	Lignin		Hemicellulose		Cellulose	
	Sand	Catalyst	Sand	Catalyst	Sand	Catalyst
Product yield (wt.%)						
Gas	44.5	45.8	47.3	57.4	55.3	60.6
Liquid	25.0	17.0	44.0	28.0	39.0	25.0
Solid	39.0	39.0	18.0	18.0	13.0	13.0
Carbon Balance (%)						
Gas	11.95	13.19	16.03	33.34	21.85	35.00
Solid	51.13	51.13	35.27	35.27	24.57	24.57
Gas ratios						
CH <sub>4</sub> /CO	0.84	1.64	0.38	4.50	0.26	3.39
CH <sub>4</sub> /CO <sub>2</sub>	2.18	5.12	0.52	3.90	4.36	3.78
Gas composition (vol.% H <sub>2</sub> free basis)						
CH <sub>4</sub>	35.8	53.5	17.2	67.6	13.3	64.2
CO	42.5	32.5	43.5	15.0	50.3	18.9
CO <sub>2</sub>	16.4	10.4	32.5	17.4	30.6	16.9
CnHm	5.2	3.6	6.4	ND	5.7	ND

ND; Not detected

**Table 4.** Mass balance and gas composition of the gases from pyrolysis-catalytic hydrogenation of biomass components with varied lignin percentage in the mixture.

	<b>Biomass component Percentages (%)</b>			
	<b>100 % lignin</b>	<b>60 wt.% lignin 20 wt.% cellulose 20 wt.% hemicellulose</b>	<b>40 wt.% lignin 30 wt.% cellulose 30 wt.% hemicellulose</b>	<b>20 wt.% lignin 40 wt.% cellulose 40 wt.% hemicellulose</b>
<b>Product yield (wt.%)</b>				
Gas	45.8	57.4	55.9	59.8
Liquid	17.0	34.0	30.0	35.0
Solid	39.0	31.0	26.0	22.0
<b>Carbon Balance (%)</b>				
Gas	13.19	23.35	24.75	29.64
Solid	51.13	46.98	42.32	34.66
<b>Gas ratios</b>				
CH <sub>4</sub> /CO	0.84	3.01	3.1	2.98
CH <sub>4</sub> /CO <sub>2</sub>	2.18	4.71	4.8	4.78
<b>Gas composition (vol.% H<sub>2</sub> free basis)</b>				
CH <sub>4</sub>	35.8	63.4	64.2	64.0
CO	42.5	21	20.9	21.4
CO <sub>2</sub>	16.4	13.5	13.4	13.3
C <sub>n</sub> H <sub>n</sub>	5.2	2.1	1.5	1.5

**Table 5.** Product yield and volumetric gas composition of the gases from pyrolysis-catalytic hydrogenation of agricultural waste biomasses.

<b>Agriculture Waste Biomass</b>				
	<b>Willow</b>	<b>Sugar cane Bagasse</b>	<b>Rice Straw</b>	<b>Ugu Plant</b>
Product yield (wt.%)				
Gas	60.4	59.3	54.7	53.4
Liquid	28.0	32.0	18.0	28.0
Solid	23.0	23.0	28.0	27.0
Gas ratios				
CH <sub>4</sub> /CO	5.3	5.5	5.6	6.5
CH <sub>4</sub> /CO <sub>2</sub>	4.0	3.6	3.8	3.8
Gas composition (vol.% H <sub>2</sub> free basis)				
CH <sub>4</sub>	68.7	68.2	68.1	69.7
CO	12.9	12.3	12.2	10.8
CO <sub>2</sub>	17.5	18.9	17.8	18.5
C <sub>n</sub> H <sub>n</sub>	0.9	0.6	1.9	1.0

## SUPPLEMENTARY INFORMATION

### Pyrolysis-Catalytic Hydrogenation of Cellulose-Hemicellulose-Lignin and Biomass Agricultural Wastes for Synthetic Natural Gas Production.

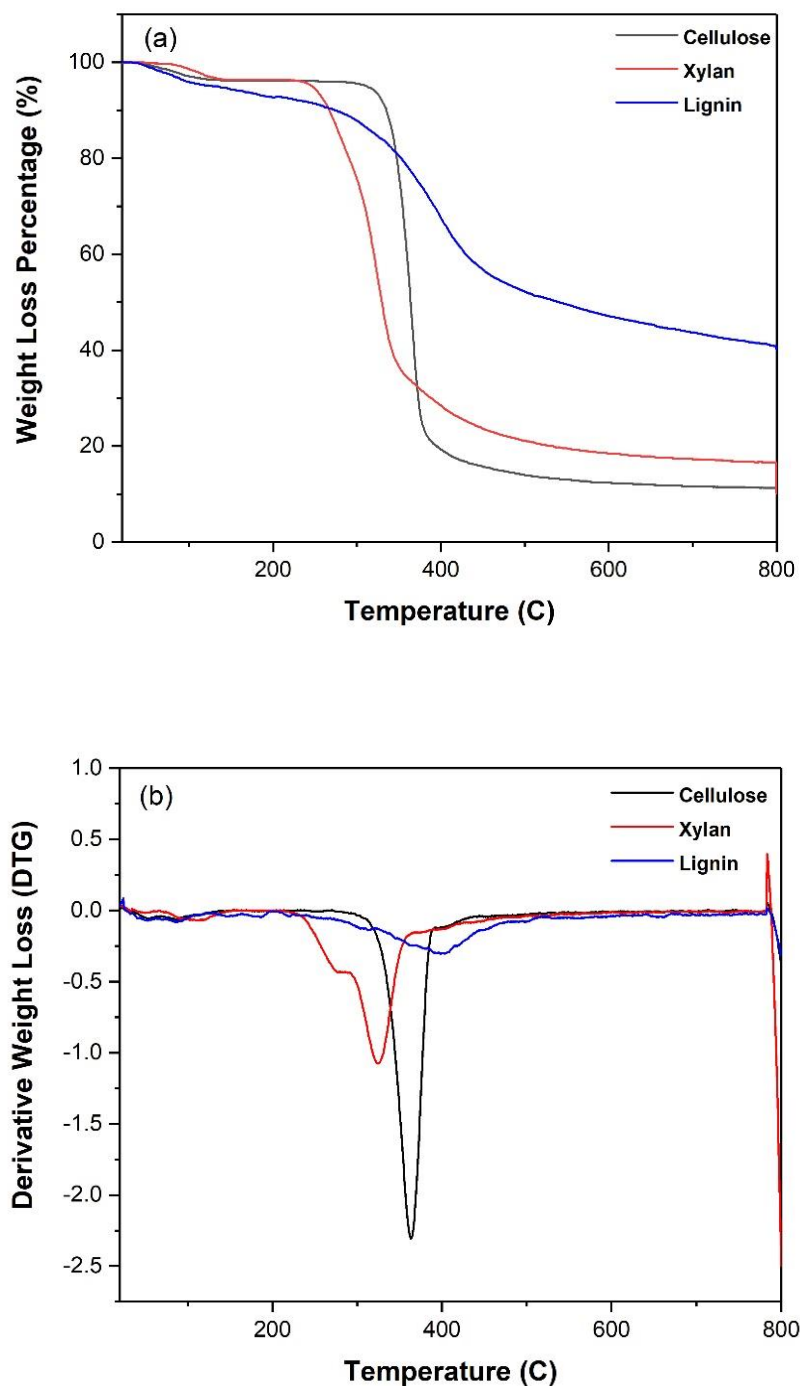


**Figure SI 1(a)** TGA and **SI 1(b)** DTG thermograms of cellulose, hemicellulose and lignin (heating rate 20 °C min<sup>-1</sup>).